

A study of possible temporal and latitudinal variations in the properties of the solar tachocline

Sarbani Basu¹ and H. M. Antia²

¹ *Astronomy department, Yale University, P.O. Box 208101 New Haven CT 06520-8101, U. S. A.*

² *Tata Institute of Fundamental Research, Homi Bhabha Road, Mumbai 400 005, India*

Accepted . Received

ABSTRACT

Temporal variations of the structure and the rotation rate of the solar tachocline region are studied using helioseismic data from the Global Oscillation Network Group (GONG) and the Michelson Doppler Imager (MDI) obtained during the period 1995–2000. We do not find any significant temporal variation in the depth of the convection zone, the position of the tachocline or the extent of overshoot below the convection zone. No systematic variation in any other properties of tachocline, like width, etc., is found either. Possibility of periodic variations in these properties is also investigated. Time-averaged results show that the tachocline is prolate with a variation by about $0.02R_{\odot}$ in its position. The depth of the convection zone or the extent of overshoot does not show any significant variation with latitude.

Key words: Sun: oscillations – Sun: interior – Sun: rotation

1 INTRODUCTION

Helioseismic data allow us to probe the structure and rotation rate of the solar interior (Gough et al. 1996; Thompson et al. 1996; Schou et al. 1998). With the accumulation of Global Oscillation Network Group (GONG) and Michelson Doppler Imager (MDI) data over the last five years, it has also become possible to study temporal variations in the rotation rate and other properties of the solar interior. It is generally believed that the solar dynamo operates in the region just below the convection zone, which is also the region where the tachocline is located (Kosovichev 1996; Basu 1997). The tachocline is defined to be the region where the rotation rate undergoes a transition from differential rotation in the convection zone to almost uniform rotation in the radiative interior (Spiegel & Zahn 1992). As a result, one would expect temporal variations associated with solar cycle to manifest in this region. However, no definite changes have been detected in these layers (Basu & Antia 2000a). Recently, Howe et al. (2000) have reported a 1.3 year periodicity in variation of equatorial rotation rate at $r = 0.72R_{\odot}$. It is not clear if this period is associated with solar cycle related variations, or indeed why it should manifest only in a narrow latitude and radius range. Using similar data, Antia & Basu (2000) did not find any periodic or systematic changes in rotation rate in the tachocline region. But both these studies are based on inversions of data to obtain the rotation rate. This process is not very reliable in the tachocline region where the steep gradient in the rotation rate tends to be smoothed by regularisation applied in inversion techniques (Gough & Thompson

1991; Antia, Basu & Chitre 1998). The properties of the solar tachocline have been studied using forward modelling techniques (Kosovichev 1996; Basu 1997; Antia et al. 1998; Charbonneau et al. 1999), which are probably better suited to account for the steep variation in rotation rate. Corbard et al. (1998, 1999) have modified inversion technique to account for sharp changes in the rotation rate. Using a simple calibration technique to study the tachocline, Basu & Schou (2000) found that the magnitude of the jump in the rotation rate across the tachocline increases with solar activity. This result needs to be checked using other techniques and with more data that are now available.

In this work, we attempt to use forward modelling techniques described by Antia et al. (1998) to study whether different properties of the tachocline vary with time. We also look for possible periodic changes in the rotation rate around the tachocline. In addition, we also study possible temporal changes in solar structure in that region, in particular, changes in the depth of the convection zone and the extent of overshoot below the convection zone. Since the depth of the convection zone can be measured very accurately – with statistical error of the order of $0.0001R_{\odot}$ – it should be possible to detect even small variations in the structure of this region.

Apart from temporal variations in the properties of the tachocline, we also attempt to find latitudinal variations in the position and the thickness of the tachocline. Antia et al. (1998) did not find any significant latitudinal variation in the position or thickness of the tachocline. Although, the results did show that the tachocline shifts upwards with latitude, this shift was comparable to the error estimates. Char-

bonneau et al. (1999) found that the mean position of the tachocline moves upwards with latitude. They found a shift of $(0.024 \pm 0.004)R_{\odot}$ in tachocline position between the latitudes of 0° and 60° , which is comparable to the upper limit on its variation given by Antia et al. (1998). With the accumulation of data over 5 years it may be possible to find out if this latitudinal variation is statistically significant. Similarly, there are some indications that the thickness of tachocline increases with latitude (Antia et al. 1998; Charbonneau et al. 1999) but this variation is not statistically significant, at least, in the results obtained so far. Thus it is of interest to check if this variation can be confirmed with longer data set.

If the position of the tachocline varies with latitude, then a natural question is whether the depth of the convection zone also varies with latitude. The relative position of the tachocline and the convection zone base plays a crucial role in the theory of the tachocline. Gough & Kosovichev (1995) using data from Big Bear Solar Observatory (Woodard & Libbrecht 1993) have claimed a decrease by about $0.02R_{\odot}$ in depth of the convection zone between the equator and latitude of 60° . This is comparable to latitudinal variations in the tachocline as found by Charbonneau et al. (1999). However, such a large variation would yield a strong signal in the even-order splitting coefficients because of the resulting asphericity. Antia et al. (2000a) did not find any significant signal in asphericity around the base of the convection zone, although they did not specifically look for a signal from varying depth of convection zone. Monteiro & Thompson (1998) attempted to detect latitudinal dependence in depth of convection zone and extent of overshoot below the convection zone, but the results were not conclusive. Similarly, Basu (1997) and Antia et al. (2000b) attempted to look for any possible magnetic field near the base of the convection zone, using the even order splitting coefficients, but once again no signal was found in the observed data. We therefore, try to check for any latitudinal variation in the depth of convection zone.

2 THE DATA

We use data for GONG months 1–46 to determine the rotation rate and the spherically symmetric structure in the solar interior. Each of these data sets covers a period of 108 days. We have used only the non-overlapping sets of data for most of the work to ensure that each data set is independent. Each GONG month covers a period of 36 days with month 1, starting on 1995 May 7 and month 46 ending on 1999 November 17. There are 15 non-overlapping data sets covering this period, and these have been used to study the temporal variations in rotation rate and structure. However, for studying the oscillatory changes in rotation rate we have also used all data sets even though they overlap in time. There are 44 data sets centered on GONG months 2–45. The data were obtained from the GONG Data Storage and Distribution System. In order to provide an independent test of the results, we also use the data from MDI. Each of these 18 data sets was obtained from 72 non-overlapping days of observations covering a period from 1996 May 1 to 2000 April 9 with some gaps corresponding to period when the Solar and Heliospheric Observatory (SOHO), the space-craft on which MDI is located, was not operational.

All these data sets (GONG and MDI) contain both the mean frequencies and splitting coefficients for the observed p-modes. The GONG data are described by Hill et al. (1996), while the MDI data are described by Schou (1999). The frequency of an eigenmode of a given degree ℓ , a given radial order n , and a given azimuthal order m can be expressed in terms of these splitting coefficients using the expansion

$$\nu_{n\ell m} = \nu_{n\ell} + \sum_{j=1}^{j_{\max}} a_j(n, \ell) \mathcal{P}_j^{(\ell)}(m), \quad (1)$$

where $\nu_{n\ell}$ is the mean frequency of the (n, ℓ) multiplet, $a_j(n, \ell)$ are the splitting coefficients and $\mathcal{P}_j^{(\ell)}(m)$ are orthogonal polynomials in m (Ritzwoller & Lavelly 1991; Schou, Christensen-Dalsgaard & Thompson 1994). There is some ambiguity in the normalisation of the polynomials $\mathcal{P}_j^{(\ell)}(m)$. We have used the definition given by Schou et al. (1994). The odd splitting coefficients, a_1, a_3, \dots , are determined by rotation rate in solar interior and have been used to infer the rotation rate as a function of depth and latitude. While the even splitting coefficients a_2, a_4, \dots are determined by magnetic fields and other aspherical perturbations in solar interior, as well as by second order effects of rotation (Gough & Thompson 1990). The even splitting coefficients can be used to study the latitudinal variations in the solar structure. For the purpose of this work we have used only modes with frequencies between 1500 and 3500 μHz .

3 THE TECHNIQUE

3.1 Depth of the convection zone

To detect possible changes in solar structure around the base of the convection zone, we determine the depth of the convection zone using the mean frequencies of the p-modes. In lower part of the convection zone the temperature gradient equals the adiabatic temperature gradient, while below the convection zone base the temperature gradient is radiative. The difference in the temperature gradient below and above the base of the convection zone introduces a characteristic feature in the sound speed difference between two models (or between a model and the Sun) if they have different convection zone depths. This signal can be used to determine this depth and we use the method described by Basu and Antia (1997) for this purpose.

We use the even-order splitting coefficients, which can be used to analyse departures from spherical symmetry (Gough 1993), to determine possible latitude-dependence of the depth of the convection zone. For simplicity, we only consider axisymmetric perturbations (with the symmetry axis coinciding with the rotation axis) that are symmetric about the equator. In this case, using the variational principle, the difference in frequency between the Sun and a solar model for a mode of a given order, degree and azimuthal order (n , ℓ , and m) can be written as:

$$\frac{\delta\nu_{n\ell m}}{\nu_{n\ell m}} = \int_0^R dr \int_0^{2\pi} d\phi \int_0^{\pi} \sin\theta d\theta \left(\mathcal{K}_{c^2, \rho}^{n\ell}(r) \frac{\delta c^2}{c^2}(r, \theta) + \mathcal{K}_{\rho, c^2}^{n\ell}(r) \frac{\delta\rho}{\rho}(r, \theta) \right) Y_{\ell}^m(Y_{\ell}^m)^*, \quad (2)$$

where r is radius, θ is colatitude, $\mathcal{K}_{c^2, \rho}^{n\ell}(r)$ and $\mathcal{K}_{\rho, c^2}^{n\ell}(r)$ are the kernels for spherically symmetric perturbations (Antia

& Basu 1994), Y_ℓ^m are spherical harmonics denoting the angular dependence of the eigenfunctions for spherically symmetric star. The relative difference in squared sound speed, $\delta c^2/c^2$ and density, $\delta\rho/\rho$ between the Sun and a solar model can be expanded in terms of even order Legendre polynomials:

$$\begin{aligned}\frac{\delta c^2}{c^2}(r, \theta) &= \sum_k c_k(r) P_{2k}(\cos \theta), \\ \frac{\delta\rho}{\rho}(r, \theta) &= \sum_k \rho_k(r) P_{2k}(\cos \theta),\end{aligned}\quad (3)$$

where $c_k(r)$ and $\rho_k(r)$ are shorthand notations for $(\delta c^2/c^2)_k(r)$ and $(\delta\rho/\rho)_k(r)$, respectively. The spherically symmetric component ($k = 0$) causes frequency differences that are independent of m and thus only contribute to the mean frequency of the (n, ℓ) multiplet. Higher order terms give frequencies that are functions of m and thus contribute to the splitting coefficients.

The angular integrals in Eq. (2) can be evaluated to give

$$\begin{aligned}\int_0^{2\pi} d\phi \int_0^\pi \sin \theta d\theta Y_\ell^m (Y_\ell^m)^* P_{2k}(\cos \theta) \\ = \frac{1}{\ell} Q_{\ell k} \mathcal{P}_{2k}^{(\ell)}(m),\end{aligned}\quad (4)$$

where $Q_{\ell k}$ depends only on ℓ, k and $\mathcal{P}_{2k}^{(\ell)}(m)$ are the orthogonal polynomials defined by Eq. (1). The extra factor of $1/\ell$ ensures that $Q_{\ell k}$ approach a constant value at large ℓ . Thus with this choice of expansion [Eq. (3)] the inversion problem is decomposed into independent inversions for each even splitting coefficient and $c_k(r), \rho_k(r)$ can be computed by inverting the splitting coefficient a_{2k} . This would be similar to the 1.5d inversions used to determine rotation rates (Ritzwoller & Lavelly 1991), called so because a two dimensional solution is obtained as a series of one dimensional inversions:

$$\frac{\ell a_{2k}(n, \ell)}{\nu_{n\ell} Q_{\ell k}} = \int_0^R \mathcal{K}_{c^2, \rho}^{n\ell} c_k(r) dr + \int_0^R \mathcal{K}_{\rho, c^2}^{n\ell} \rho_k(r) dr. \quad (5)$$

To determine the sound speed or density at a particular colatitude θ we can combine these solutions using Eq. (3). Thus to invert for $\delta c^2/c^2$ at colatitude θ , we can use the usual equation for spherically symmetric case with the frequency difference given by:

$$\delta\nu = \delta\nu_{n\ell} + \sum_k \frac{\ell a_{2k}(n, \ell)}{Q_{\ell k}} P_{2k}(\cos \theta), \quad (6)$$

where $\delta\nu_{n\ell}$ is the difference in mean frequency for the n, ℓ multiplet, between the Sun and a solar model. Thus with this choice of $\delta\nu$ we can apply the technique used by Basu & Antia (1997) to determine convection zone depth at a given colatitude.

3.2 Overshoot below the convection zone

In addition to the depth of the convection zone, we attempt to determine changes in the extent of overshoot below the convection zone. The sudden change in the temperature gradient at the base of the convection zone introduces an oscillatory signal in the frequencies as a function of radial order n (Gough 1990). The presence of an adiabatically stratified

overshoot layer causes the temperature gradient to have a discontinuity, the magnitude of discontinuity increasing with the extent of overshoot. Thus the amplitude of the oscillatory signal also increases with the extent of overshoot. To a first approximation, this signal has the form $A \cos(2\tau\nu + \phi)$, where ν is the frequency of the mode, τ , the ‘frequency’ of the signal is the acoustic depth of the transition layer, A is the amplitude and ϕ a phase. This signal has been used earlier to estimate the extent of overshoot below the solar convection zone (Monteiro, Christensen-Dalsgaard & Thompson 1994; Basu, Antia & Narasimha 1994). The oscillatory signal can be amplified by taking the fourth differences of the frequencies as a function of the radial order n enabling a more precise measurement of the amplitude, A , of oscillations (Basu et al. 1994). Since the amplitude of the signal increases with increase in extent of overshoot, it can be calibrated against amplitudes for models with known extents of overshoot. We use the method described by Basu (1997) to isolate the oscillatory signal and measure its characteristics. Data sets used so far indicate that the amplitude of the oscillatory signal is consistent with no overshoot, however, this does not preclude any change of the amplitude with time. The precision of this measurement is much less than that of the depth of the convection zone, but since there is some suggestion that this amplitude may be varying with time (Monteiro et al. 1998) it needs to be checked independently.

We can also calculate the latitude dependence of extent of overshoot by adding the contribution from even splitting coefficients as given in Eq. (6) to the frequencies. The resulting frequencies can be used to calculate the fourth difference and the oscillatory part can be isolated as explained above to calculate the amplitude. Any variation in amplitude of this oscillatory signal can be attributed to change in extent of overshoot with latitude. Since the errors in estimating the extent of overshoot are much larger than those in estimating the depth of the convection zone, probability of detecting either temporal or latitudinal variation in extent of overshoot is much smaller than those in convection zone depth. But for completeness we have attempted to study this variation too.

3.3 The tachocline

To determine the properties of tachocline we use the three techniques described by Antia et al. (1998), which are (1) a calibration method in which the properties at each latitude are determined by direct comparison with models; (2) a one dimensional (henceforth, 1d) annealing technique in which the parameters defining the tachocline at each latitude are determined by a nonlinear least squares minimization using simulated annealing method and (3) a two-dimensional (henceforth, 2d) annealing technique, where the entire latitude dependence of tachocline is fitted simultaneously, again using simulated annealing. The properties we are interested in are the position and the thickness of the tachocline and the change in rotation rate across the tachocline. We study these properties as a function of latitude using all the techniques listed above. The use of three different techniques allows us a check on the results. In all techniques the tachocline is represented by a model of the

form (cf., Antia et al. 1998),

$$\Omega_{\text{tac}} = \frac{\delta\Omega}{1 + \exp[(r_t - r)/w]}, \quad (7)$$

where $\delta\Omega$ is the jump in the rotation rate across the tachocline, w is the half-width of the transition layer, and r_t the radial distance of the mid-point of the transition region. A positive value of $\delta\Omega$ implies that the rotation rate in the convection zone is larger than that in the radiative zone. The quantities $\delta\Omega$, w and r_t could be a function of latitude. It should be noted that the model for tachocline used by us is different from that used by Kosovichev (1996) or Charbonneau et al. (1999) and in particular, the definition of width in the two models is significantly different (see Antia et al. 1998). For the annealing techniques a model for smooth part of the rotation rate is also required and we use the same model as that used by Antia et al. (1998):

$$\Omega(r) = \begin{cases} \Omega_c + B(r - 0.7) & \text{if } r \leq 0.95 \\ \Omega_c + 0.25B - C(r - 0.95) & \text{if } r > 0.95. \end{cases} \quad (8)$$

Here r is the radius in units of solar radius, Ω_c is the rotation rate in radiative interior, B is the average gradient of the rotation rate in lower part of the convection zone and C is the average gradient in the near surface shear layer.

4 RESULTS

4.1 Depth of the convection zone

We calculate the position of the base of the convection zone (r_d) using the frequencies from each data set from GONG and MDI and the results are shown in Fig. 1. The error bars shown in Fig. 1 represent uncertainties due to those in the data, i.e., statistical errors. There are systematic errors which can be up to a factor of five larger than the statistical errors (Basu 1998). The systematic error for each data set should be the same and hence does not affect any conclusion about variations with time. There is very good agreement between results obtained using GONG and MDI data. There does not appear to be any systematic pattern in these temporal variations. There are some oscillations in these values as a function of time. In order to check for possible periodicities we take the Fourier transform of $r_d(t)$ and we do not see any significant peak in the resulting power spectrum at any frequency. Thus the variations do not appear to be periodic. The temporal average over all the 33 data sets from GONG and MDI gives $r_d = (0.71336 \pm 0.00002)R_\odot$, which agrees well with the earlier estimates of Christensen-Dalsgaard, Gough & Thompson (1991), Basu & Antia (1997) and Basu (1998).

The lower panel in Fig. 1 shows the results plotted against the mean 10.7 cm Radio flux during the time interval covered by each data set as obtained from the Solar Geophysical data web page (www.ngdc.noaa.gov/stp/stp.html) of the US National Geophysical Data Center. The 10.7 cm flux from the Sun is known to track solar activity. There does not appear to be any correlation between the position of convection zone base and the 10.7 cm flux. In fact, the correlation coefficient between these quantities is only -0.18 . All these results suggest that there is no systematic variation in the depth of the convection zone with solar activity.

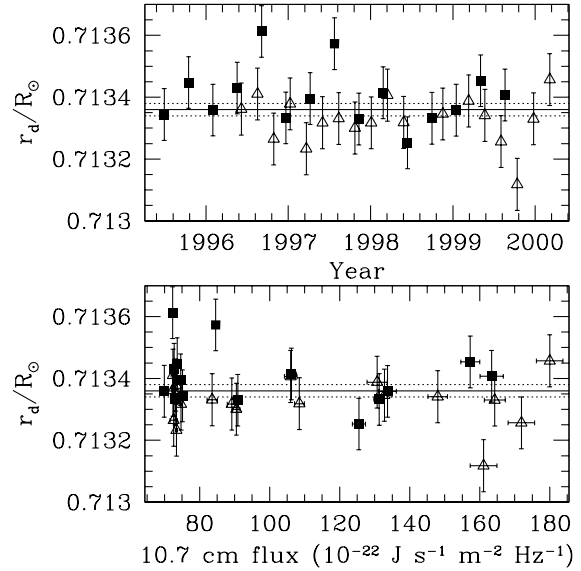


Figure 1. The position of the base of the solar convection zone plotted as a function of time and the 10.7 cm radio flux, which is an indicator of solar activity. The squares represent GONG and triangles denote MDI data. The continuous, horizontal line is the average of all the results, with the 1σ limits marked by dotted lines.

An upper limit on any possible variation would be comparable to the error estimates in individual measurements, which is $0.0001R_\odot$ or 70 km. To get a better limit on any possible variation in the depth of the CZ with solar activity, we divided the data into two groups, those with 10.7 cm flux lower than 100 flux units (the unit being $10^{-22} \text{ J s}^{-1} \text{ m}^{-2} \text{ Hz}^{-1}$) and those with 10.7 cm flux of above 120 flux units. Nine data sets each from GONG and MDI fall into the first category, and seven MDI sets and five GONG sets fall into the second category. The low activity data sets indicate that the CZ base is at $r_d = (0.71337 \pm 0.00002)R_\odot$, the higher activity set gives $r_d = (0.71333 \pm 0.00003)R_\odot$. Thus the variation in convection zone depth is about (28 ± 25) km, between these sets with mean 10.7 cm flux of 77.2 ± 7.1 and 150.0 ± 18.7 flux units, respectively.

As explained in Section 3.1, we can calculate the depth of the convection zone at different latitudes using the even order splitting coefficients. We have calculated r_d at several different latitudes for all the data sets and these results also do not show any significant temporal variation at any latitude. In this case, the error estimates are larger and hence the corresponding upper limit on possible temporal variations would also be larger.

4.2 Overshoot below the convection zone

We have used all independent data sets available to us to check whether there is any temporal variation in the extent of overshoot below the solar convection zone. For this purpose we use frequencies for p -modes with $5 \leq \ell \leq 20$ and $2 \leq \nu \leq 3.5$ mHz. Figure 2 shows the mean amplitude, A , of the oscillatory part in the fourth difference of the frequencies due to the transition at the base of the overshoot layer, as a function of time. This amplitude would be related to

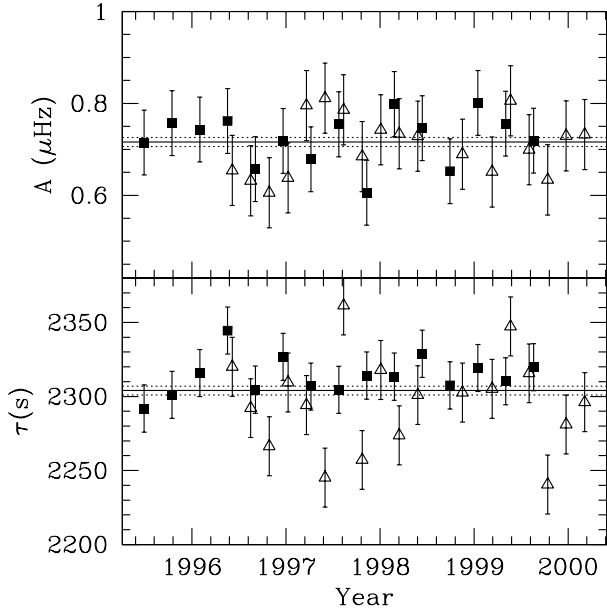


Figure 2. The amplitude, A and the frequency, τ of the oscillatory signal in the fourth difference of frequencies plotted as a function of time for GONG (squares) and MDI (triangles) data. The continuous, horizontal line is the average of all the results, with the 1σ limits marked by dotted lines.

the extent of overshoot below the convection zone. There is good agreement between the results obtained using GONG and MDI data sets. Once again there is no clear trend and the oscillatory features are not periodic. The time-average of the amplitude as obtained from averaging over result from all sets is $0.716 \pm 0.010 \mu\text{Hz}$, which is in reasonable agreement with the earlier results obtained by Basu et al. (1994) and Basu (1997). This amplitude is significantly less than that in a solar model without overshoot below the convection zone ($A = 0.805 \mu\text{Hz}$). The frequencies in both GONG and MDI data have been calculated by assuming that the peak profiles in power spectra are symmetric. However, it is well known that the peaks are actually asymmetric and use of symmetric peak profiles causes frequencies to be shifted away from true value. Basu and Antia (2000b) found that the use of symmetric profile tends to underestimate the amplitude of the oscillatory signal. This may explain the apparent contradiction that the amplitude for observed data is significantly smaller than that in a solar model without overshoot. If we assume that the use of asymmetric profile increases the amplitude by the same amount as that found by Basu and Antia (2000b) then the resulting amplitude will be consistent with that in a solar model without overshoot.

Figure 2 also shows how the frequency, τ of the oscillatory part in frequencies due to the transition at the base of the overshoot layer changes as a function of time. This frequency is expected to be the acoustic depth of the base of overshoot layer. Once again we do not see any systematic variation in the acoustic depth with time. The average of the results obtained using all 33 data sets is $\tau = 2304 \pm 3$ s, which is in reasonable agreement with the earlier results obtained by Basu et al. (1994) and Basu (1997).

As explained in Section 3.2 we can also calculate the extent of overshoot at different latitudes, using the information from even splitting coefficients. But in this case the

errors are too large and it is difficult to isolate the small oscillatory signal and hence no definitive results could be obtained. However, we may not expect any time-variation in the overshoot results since the depth of the convection zone, which can be determined much more accurately, also doesn't show any temporal variation of either the spherically symmetric value or values at individual latitudes.

4.3 Temporal variations in the tachocline

Having failed to find any systematic temporal variations in the spherically symmetric structure near the base of the convection zone, we attempt to look for variations in the rotation rate that define the tachocline. Using each data set from GONG and MDI we determine the position, width and jump across the tachocline using all the three techniques mentioned in Section 3.3. For this purpose we use only those modes which have lower turning points in the range $0.6-0.9R_{\odot}$. The results at a few selected latitudes are shown in Figs. 3–5. There is a general agreement between different techniques and data sets, as all the results are within respective error estimates. However, some systematic differences between different data sets and techniques can be seen, particularly at high latitudes. These differences are comparable to error estimates in individual values but if temporal mean is taken over all values the differences could be significant. The origin of these systematic differences is not clear. There is no systematic temporal variation in either the position or the width of the tachocline in any of the results. From Fig. 3, it is clear that there is some latitudinal variation in the position of the tachocline as the mean position moves upwards with latitude. We will discuss this latitudinal variation in the next subsection. The jump in the rotation rate across the tachocline obtained by the calibration method appears to show a steady increase with time at low latitudes, as was seen by Basu & Schou (2000) using the same technique. The increase however, is comparable to error limits and is not seen in results obtained from annealing technique. Hence the significance of this trend is not clear. This trend is not very clear even in results obtained using calibration method at latitudes of 45° and 60° .

The values of the jump in the rotation rate across the tachocline obtained using the 2d annealing technique appear to show an oscillatory behaviour at low latitudes. This can be traced back to oscillations in the latitudinally independent component of jump. Following Antia et al. (1998), $\delta\Omega$ in the 2d annealing technique can be expanded as

$$\delta\Omega(\theta) = \delta\Omega_1 + \delta\Omega_3 P_3(\theta) + \delta\Omega_5 P_5(\theta), \quad (9)$$

where

$$\begin{aligned} P_3(\theta) &= 5 \cos^2 \theta - 1, \\ P_5(\theta) &= 21 \cos^4 \theta - 14 \cos^2 \theta + 1. \end{aligned} \quad (10)$$

Fig. 6 shows the three components obtained from GONG and MDI data as a function of time. There are some oscillations in the first component $\delta\Omega_1$ which appear to be similar to that seen by Howe et al. (2000) in the equatorial rotation rate at $r = 0.72R_{\odot}$. It may be noted that we see these oscillations in the spherically symmetric component which is independent of latitude and its phase is also different from that found by Howe et al. (2000). In order to check the significance of these oscillations we need to look at other

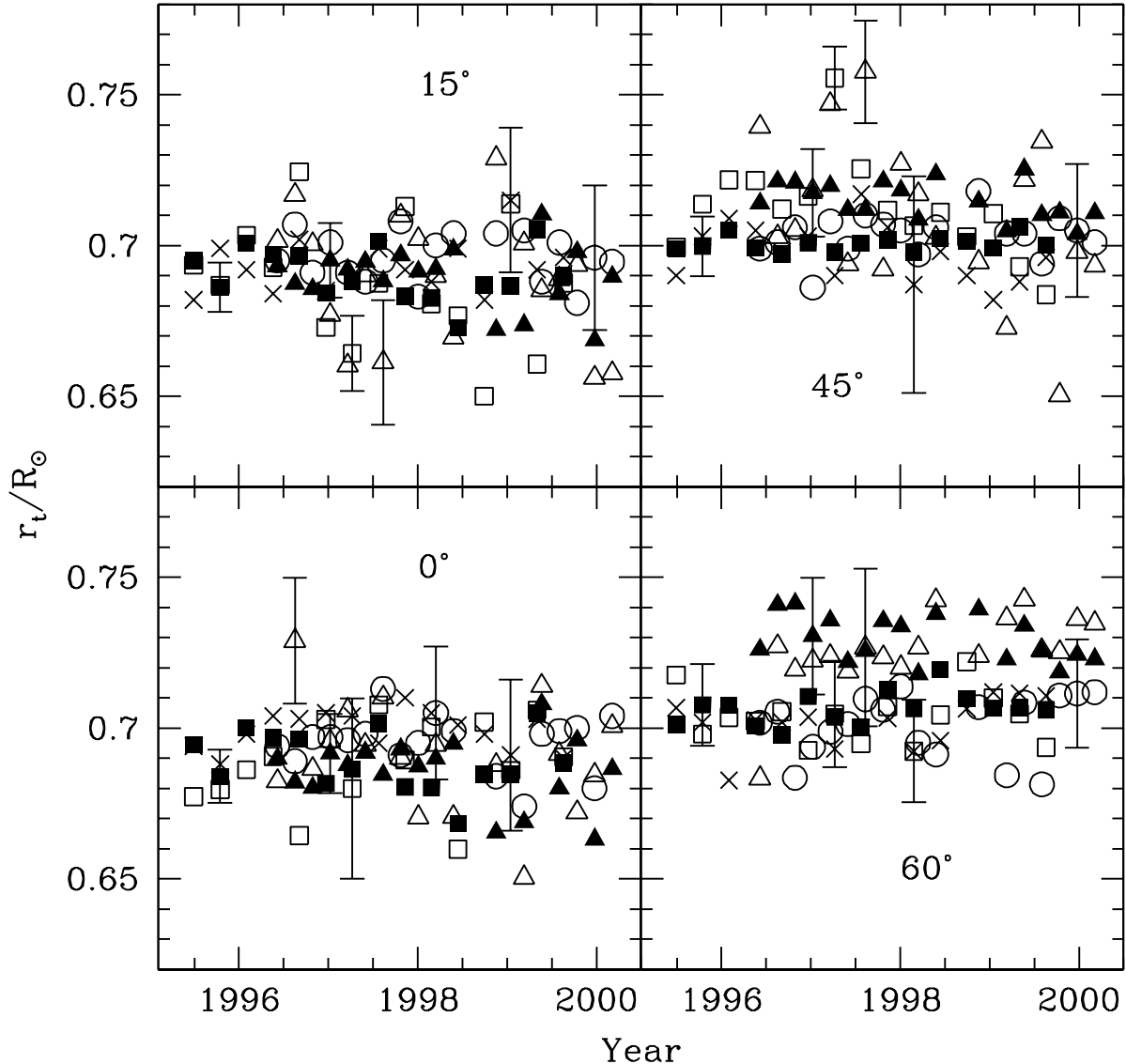


Figure 3. The mean radial position of the tachocline at a few selected latitudes. The crosses and circles show the results from calibration method for GONG and MDI data, the open squares and triangles show the 1d annealing results from GONG and MDI data, while the filled squares and triangles show the results from 2d annealing for GONG and MDI data. For clarity only one representative error-bar is shown for each technique.

parameters fitted in 2d annealing method. It turns out that $\delta\Omega_1$ is anti-correlated with Ω_c , the rotation rate in the radiative zone below the tachocline. This anti-correlation is due to the fact that it is difficult to distinguish between the effects of these two parameters in the tachocline model that is used for fitting. This behaviour is caused by the fact that the jump in the spherically symmetric component of the rotation rate across the tachocline is very small and as a result, it is difficult to distinguish between the sharp gradient of the rotation rate in the tachocline region and the smoother gradient in the convection zone. Figure 7 shows Ω_c as well as the sum $\Omega_c + \delta\Omega_1$, which is the spherically symmetric component of rotation rate just above the tachocline. It can be seen that the variations in $\Omega_c + \delta\Omega_1$ are much less than those in either Ω_c or $\delta\Omega_1$.

In order to test if the oscillatory variation in $\delta\Omega_1$ or Ω_c

are periodic, we take the Fourier transform of these results (after subtracting out the temporal mean) and the resulting power spectra are shown in the lower panel of Fig. 7. It is clear that the spectra of $\delta\Omega_1$ and Ω_c from GONG data shows a moderately clear peak around a frequency of 0.7 yr^{-1} or a period of 1.4 years. This is comparable to the period found by Howe et al. (2000) but the peak is rather broad and not very significant statistically. The 1σ error estimates on these peaks turns out to be larger than the peak height and hence these peaks are not likely to be significant. Moreover, the peak is not clearly present in MDI data. The Fourier spectrum of MDI results shows two peaks at frequencies of 0.6 and 0.9 yr^{-1} , with the second peak being more dominant. The combination $\Omega_c + \delta\Omega_1$ does not show any clear peak for either GONG or MDI data. Hence, this spectrum is not shown in the figure.

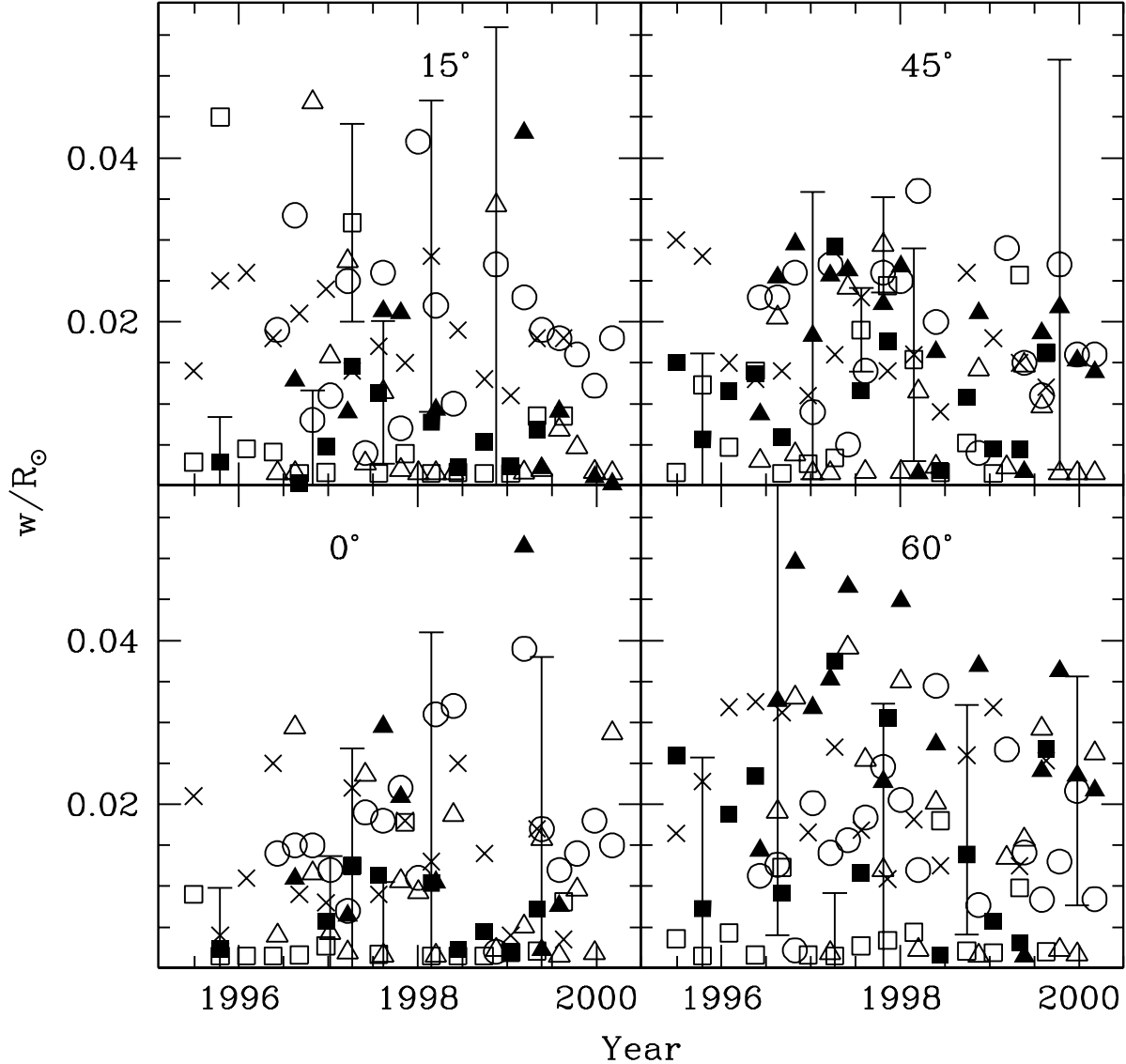


Figure 4. The width of the tachocline at a few selected latitudes. The different styles of the points have the same meaning as in Fig. 3.

Since the latitudinally independent component of rotation rate should contribute only to the splitting coefficient a_1 , we also try to fit a_1 separately to check if the oscillations are present. Furthermore, following Howe et al. (2000) we fit all GONG data sets centered at GONG months 2–45, including those that overlap in time. Since the jump in a_1 is rather small it is not possible to fit all the parameters used to define the tachocline using a_1 alone. We, therefore, keep the position and half-width of tachocline fixed at representative values of $0.69R_\odot$ and $0.009R_\odot$ to obtain other parameters including $\delta\Omega_1$ and Ω_c . These results are shown in Fig. 8. We have verified that these results are not sensitive to the choice of position and thickness. The oscillations in $\delta\Omega_1$ are still present in these results, though it is not clear if these are strictly periodic. There is very good agreement between GONG and MDI data points at all times and these oscillations are similar to that found by Howe et al. (2000) in equatorial rotation rate at $r = 0.72R_\odot$. The phase and amplitude of these oscillations are also similar to that found

by Howe et al. (2000). To check for periodicities we take the Fourier transform (after subtracting out the temporal mean) and the results are also shown in Fig. 8. This figure also shows the Fourier transform of results obtained from only non-overlapping sets of GONG data. It can be seen that in both cases we get similar peaks in the power spectra, thus it may not be essential to use all data sets in order to identify periodicity. However, the significance of the peaks is, of course, different when all data sets are used. The GONG and MDI spectra show a peak at frequencies around 0.8 and 0.9 yr^{-1} , respectively. The peak heights are smaller than 1σ error estimates when only non-overlapping data sets are used for GONG. The peak in the Fourier spectrum of results obtained from all GONG data sets, is about 1.5σ , but its significance is not clear since the errors are estimated by assuming that all data sets are independent, which is not the case because of the temporal overlap. Thus in all cases the significance of the peak is questionable. It may be noted that since we have data spanning about 4 years,

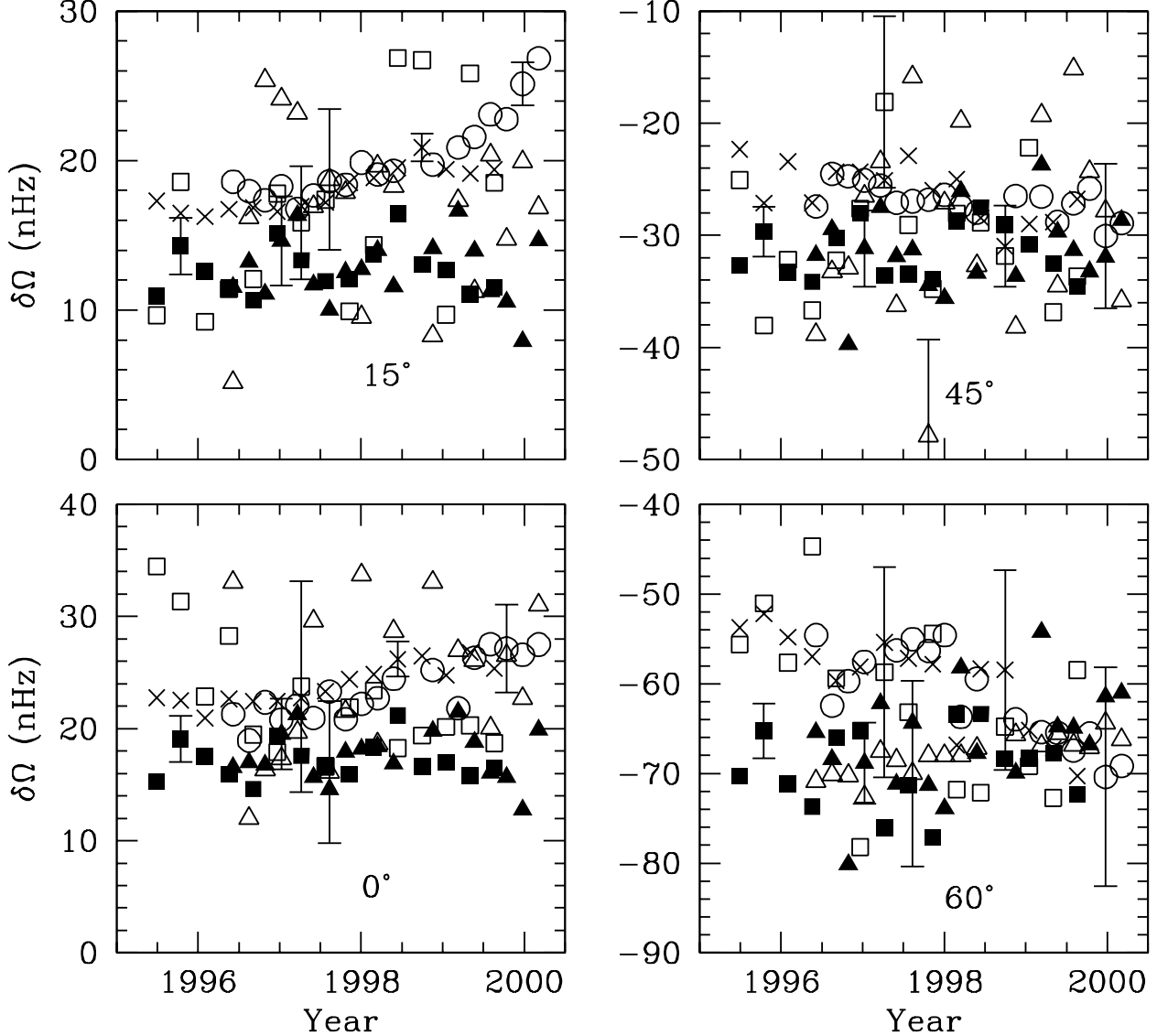


Figure 5. The jump in rotation rate across the tachocline at a few selected latitudes. The different styles of the points have the same meaning as in Fig. 3.

the frequency resolution in the power spectra is around 0.25 yr^{-1} . Hence, to within this frequency resolution the peaks in GONG and MDI spectra are close to the period of 1 year, which may arise from annual variations in the data. Both GONG and MDI data could be affected by the orbital motion of the Earth and one may expect a periodicity of 1 year in the data. Furthermore, it may be noted that the peak height has reduced by a factor of more than 3 between Figs. 7 and 8. This is approximately the square of ratio of error estimates in the two cases. This probably implies that at least, in Fig. 7, the peak is not significant. In the case of fit to only a_1 also, Ω_c and $\delta\Omega_1$ are anti-correlated and their Fourier spectra are similar.

4.4 Latitudinal variation of the Tachocline

In addition to temporal variations, we can also study latitudinal variations in the properties of the tachocline. For

this purpose we take the average of the tachocline properties obtained from all the data sets. Averaging over the 15 sets of non-overlapping GONG results obtained using the 2d annealing technique we get the following results:

$$\begin{aligned} r_t &= [(0.6936 \pm 0.0020) + (0.0047 \pm 0.0010)P_3(\theta)]R_\odot, \\ w &= [(0.0048 \pm 0.0009) + (0.0029 \pm 0.0017)P_3(\theta)]R_\odot, \\ \delta\Omega &= -(1.27 \pm 0.47) - (21.86 \pm 0.21)P_3(\theta) \\ &\quad - (3.44 \pm 0.11)P_5(\theta) \text{ nHz}. \end{aligned} \quad (11)$$

Similarly, the average over the 18 sets of MDI 2d annealing results is:

$$\begin{aligned} r_t &= [(0.6973 \pm 0.0028) + (0.0118 \pm 0.0013)P_3(\theta)]R_\odot, \\ w &= [(0.0078 \pm 0.0023) + (0.0040 \pm 0.0023)P_3(\theta)]R_\odot, \\ \delta\Omega &= -(1.17 \pm 0.68) - (21.47 \pm 0.28)P_3(\theta) \\ &\quad - (2.68 \pm 0.14)P_5(\theta) \text{ nHz}. \end{aligned} \quad (12)$$

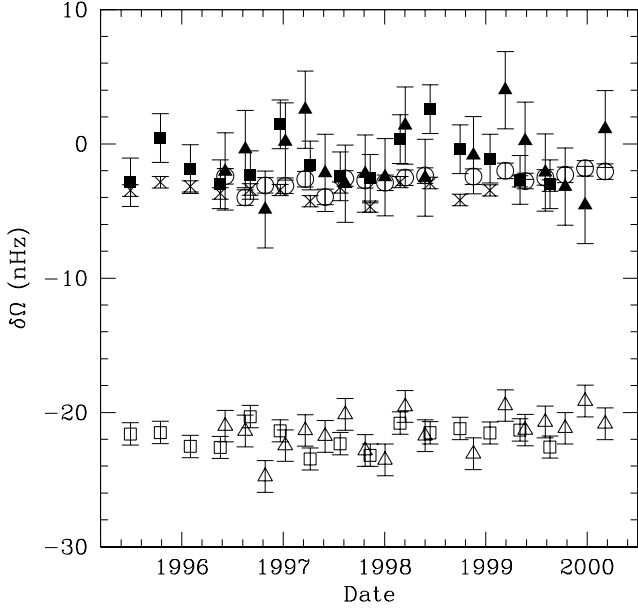


Figure 6. The three components of the jump in rotation rate across the tachocline as obtained using 2d annealing technique. The filled squares and triangles show $\delta\Omega_1$ from GONG and MDI data respectively. The open squares and triangles show $\delta\Omega_3$ from GONG and MDI data respectively, while the crosses and circles show $\delta\Omega_5$ from GONG and MDI data respectively.

These results are similar to those found by Antia et al. (1998) using a different data set from GONG. It is clear that both sets of data show significant variation in the position of the tachocline with latitude, although the extent of variation is quite different – MDI results showing much more variation than GONG results. The latitudinal variation in thickness is not significant in either set. There is clearly some systematic difference between the MDI and GONG results, particularly, in the latitudinally varying component of r_t . The origin of this difference is not clear. Other fitted parameters are in reasonable agreement between the two sets of results.

Figure 9 compares the time-averaged results of the tachocline properties obtained using different techniques and data sets as a function of latitude. It is clear that all results show that the position of the tachocline moves outwards with latitude. In fact, this trend can be seen in the individual results shown in Fig. 3 also. The latitudinal variation in width is not clear, but the results tend to suggest that the thickness increases with latitude. Though it is possible that this increase may be due to increase in errors with latitude. The jump in rotation rate across the tachocline, $\delta\Omega$, of course, shows a pronounced latitudinal variation, which is well known. In order to get better idea of latitudinal variation we take weighted average over all six measurements at each latitude and the results are shown in Table 1. Thus the increase by $0.020R_\odot$ in r_t with latitude is significantly larger than the error estimates, while the increase in half-width by $0.006R_\odot$ is only marginally significant. The shift in tachocline position with latitude is comparable to that found by Charbonneau et al. (1999). Thus our results also support the conclusion that the tachocline is prolate.

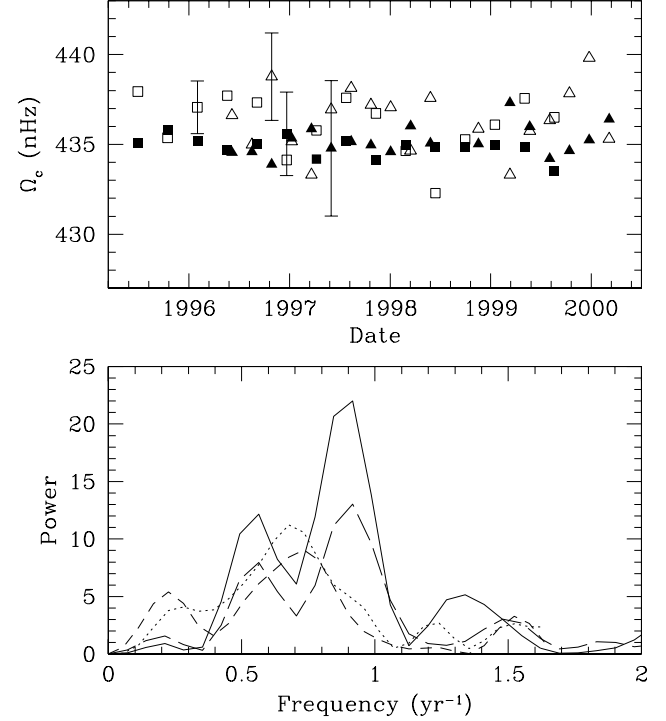


Figure 7. The upper panel shows the latitudinally averaged rotation rate in radiative interior, Ω_c and that just above the tachocline ($\Omega_c + \delta\Omega_1$) as obtained from the 2d annealing technique. The open squares and triangles represent Ω_c obtained using the GONG and MDI data respectively, while filled symbols show $\Omega_c + \delta\Omega_1$. The lower panel shows the Fourier transform of Ω_c and $\delta\Omega_1$. The continuous and dotted lines show the power in $\delta\Omega_1$ from MDI and GONG data respectively, while the long-dashed and short-dashed lines show the power in Ω_c from MDI and GONG data. Error estimates on these power spectra are not shown as the estimated error is larger than the peak heights.

Table 1. Mean properties of tachocline at different latitudes

Latitude ($^\circ$)	$\delta\Omega$ (nHz)	r_t (R_\odot)	w (R_\odot)
0	21.18 ± 0.27	0.6893 ± 0.0023	0.0061 ± 0.0012
15	17.48 ± 0.17	0.6899 ± 0.0021	0.0061 ± 0.0010
45	-30.11 ± 0.39	0.7077 ± 0.0021	0.0108 ± 0.0012
60	-67.27 ± 0.58	0.7093 ± 0.0027	0.0135 ± 0.0015

4.5 Latitudinal variation in the depth of the convection zone and extent of overshoot

Having found the tachocline to be prolate, it is of interest to check whether the base of the convection zone has the same shape. The relative position of the base of the convection zone with respect to the tachocline plays a crucial role in theoretical models to explain the formation of the tachocline. To determine the depth of the convection zone at different latitudes we construct frequency differences between a solar model and the Sun using Eq. (6) and apply the same technique as that used in Section 4.1 to determine the position of the base of the convection zone. Once again we time-average the results to determine the latitudinal variation more precisely than what we would be able to with just one set of data. The results at a few different latitudes are

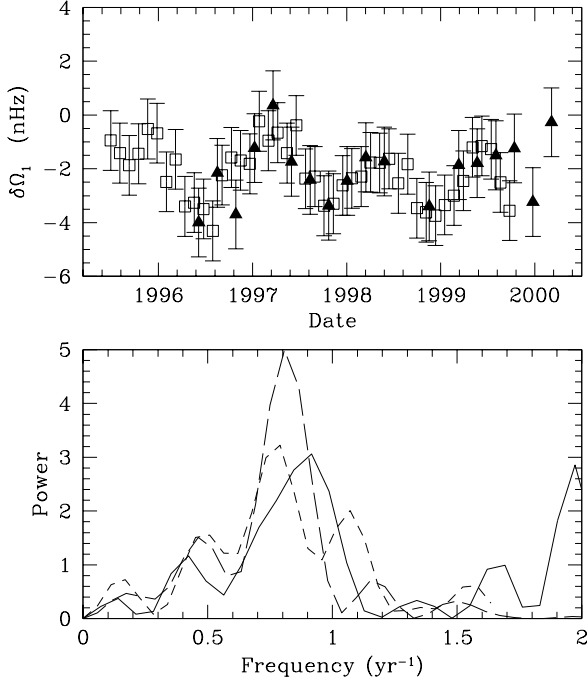


Figure 8. The upper panel shows the jump in latitudinally independent component of rotation rate across the tachocline, $\delta\Omega_1$ obtained by fitting only the splitting coefficient a_1 . The squares and triangles, respectively represent the values obtained from GONG and MDI data. The lower panel shows the Fourier transform of $\delta\Omega_1$ from MDI (continuous line) and GONG (short-dashed line) data using non-overlapping data sets, while the long-dashed line shows the spectra using all data sets from GONG.

Table 2. Mean position of base of the convection zone and extent of overshoot at different latitudes

Latitude ($^\circ$)	r_d (R_\odot)	A (μHz)	τ (s)
Mean	0.71336 ± 0.00002	0.716 ± 0.010	2304 ± 3
0	0.71333 ± 0.00010	0.889 ± 0.095	2330 ± 24
15	0.71338 ± 0.00008	0.758 ± 0.050	2314 ± 12
30	0.71334 ± 0.00008	0.905 ± 0.055	2273 ± 14
45	0.71324 ± 0.00008	0.761 ± 0.064	2329 ± 15
60	0.71359 ± 0.00013	0.602 ± 0.165	2310 ± 97
75	0.71312 ± 0.00080		

shown in Table 2. The first row in this table is the result for the spherically symmetric case. These results do not show any clear indication of latitudinal variation in the depth of the convection zone and we can put an upper limit of about $0.0005R_\odot$ on possible variations. Nevertheless, the results appear to indicate that there is a marginally significant increase in r_d around a latitude of 60° . Interestingly, Antia et al. (2000a), in their inversion results for the aspherical component of the solar sound speed, find an excess over the spherically symmetric value of the sound speed in the convection zone around this latitude. It is possible that this feature extends up to the base of the convection zone and gives rise to this small excess at 60° in r_d . More data are needed to confirm the departure from sphericity of the base of the convection zone. In any case, this difference is two orders of magnitude less than the variation claimed by Gough

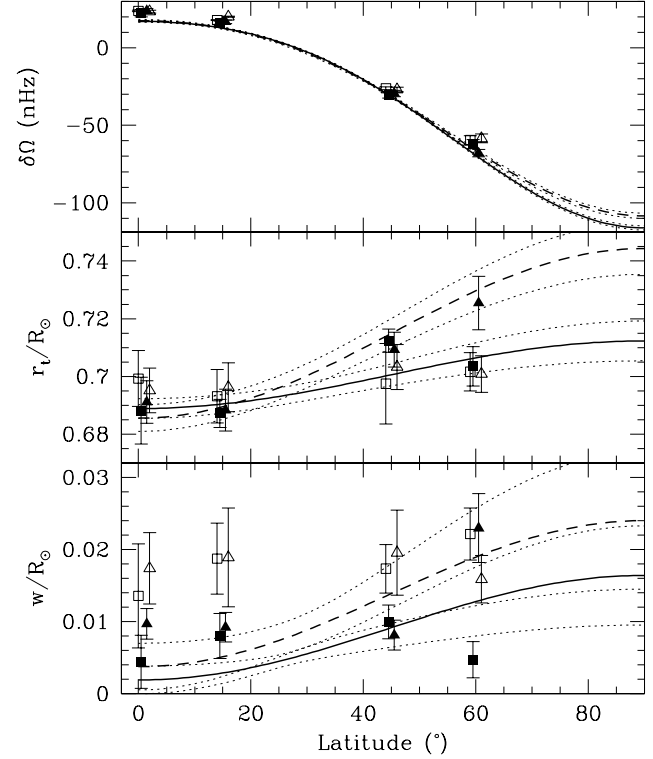


Figure 9. Temporal average of tachocline properties obtained from both GONG and MDI data. In each panel the continuous and dashed lines show the results obtained using the 2d annealing technique for GONG and MDI data respectively. The dotted lines show the error estimates on these. The squares and triangles, respectively, show the result obtained using GONG and MDI data. The filled symbols represent results obtained using 1d annealing technique, while the open symbols show results from the calibration method. These symbols are shifted by 0.5° or 1° about the true latitude for clarity.

& Kosovichev (1995). We can certainly rule out a variation of $0.02R_\odot$, which is what is seen for the tachocline position. Thus it is clear that while the tachocline has a prolate shape, the base of the convection zone is more or less spherical.

We also attempt to determine the latitudinal dependence of the extent of overshoot below the convection zone, by studying the amplitude of the oscillatory component in the fourth differences of the frequencies with appropriate combinations of even splitting coefficients added. In this case, since the errors in individual data sets are too large to isolate the oscillatory component in frequencies, we take average frequencies over all available data sets in GONG or MDI for each latitude and then study the oscillatory component in these. The results are shown in Table 2. Even after averaging over all sets, the errors are still substantial and it is not possible to get any meaningful results at high latitudes. That is why we haven't included the results at 75° latitude. There is no clear latitudinal dependence in either the amplitude, A of the oscillatory signal or its frequency, τ . The amplitude is consistent with that of a model without any overshoot. The amplitude is generally larger than what is seen for the mean spherically symmetric data, but the increase may not be significant as the amplitude tends to be overestimated when the data have substantial error (Basu 1997). Thus we do not find any evidence for latitudinal vari-

ation in the extent of overshoot below the solar convection zone.

5 DISCUSSION

Using data from GONG and MDI covering the period 1995–2000 we have tried to determine temporal variations in structure and dynamics near the base of the solar convection zone. This region is widely believed to be the seat of solar dynamo. We fail to find any significant signal of time variation, solar-cycle related or otherwise, in either the structure, or the dynamics of the base of the solar convection zone. The depth of the convection zone does not show any significant change with time, nor does the extent of overshoot. Any systematic variation in the convection-zone depth should be small, with the estimated change being 28 ± 25 km.

We do not find any convincing evidence of change in the dynamics near the solar convection zone base either. We have used three different forward modelling techniques to study the characteristics of the solar tachocline. Neither the position, nor the thickness of the tachocline show any temporal variation, while the result for the jump in the rotation rate across the tachocline depends slightly on the technique used in studying the tachocline. The results obtained by the calibration technique show a mild increase in the jump with time at low latitudes, the increase being comparable to the estimated error in the results. The annealing techniques, on the other hand, do not show any systematic increase. The 2d annealing results show some oscillatory behaviour. There is a weak periodic signal in both MDI and GONG data for $\delta\Omega_1$, the spherically symmetric component of the jump in rotation rate across the tachocline and Ω_c , the spherically symmetric component of rotation rate in the radiative interior. The Fourier transforms of $\delta\Omega_1$ or Ω_c obtained using only the splitting coefficient a_1 show peaks around a frequency of $0.8\text{--}0.9\text{ yr}^{-1}$ which are at 1σ level. The frequency resolution of the transforms is 0.25 yr^{-1} , thus these peaks are close to a period of 1 year, which may be expected from the orbital motion of the Earth. The significance of these peaks is even more unclear since the 2d annealing fits show an anti-correlation between the parameters $\delta\Omega_1$ and Ω_c . This is most probably caused by the difficulty in distinguishing between these parameters in a_1 for the model of tachocline used to fit the observed data.

We do not find any convincing evidence of 1.3 year periodicity found by Howe et al. (2000). A closer look at their figure shows that the periodic behaviour is seen clearly in only the GONG results and is not clear in the results obtained using MDI data. As such the significance of this periodicity is questionable. We do not find any significant periodicity even in the GONG data. We find a marginally significant periodicity in the spherically symmetric component of rotation rate below the tachocline. This is quite different from strong latitudinal variation claimed by Howe et al. (2000). The spherically symmetric component of rotation rate is determined using the splitting coefficient a_1 , which has to be corrected for the effects of the orbital motion of Earth. The correction from synodic to sidereal rotation rate depends on the Earth's orbital motion, and there may be some error in applying this correction. Thus one may expect a periodicity of 1 year in the observed values of a_1 . The limited frequency resolution of current data sets may cause the peak in the

Fourier spectrum to be shifted to slightly different values of the period. Were this to be true, one would expect this effect to give oscillations in Ω which are independent of depth. However, we find a depth dependence in the oscillations, and moreover, two independent data sets appear to agree with each other, suggesting a solar origin of the signal. It is quite possible that the periodic signal arising from orbital effects depends on the degree, ℓ , in which case a depth-dependence is expected. If this signal indeed represents real oscillations on the Sun, then it is not clear if it is related to solar activity or solar dynamo. Origin of such a periodicity will be difficult to understand theoretically. A periodicity with period around 1 year is also seen in the frequencies of f-modes (Antia et al. 2000, in preparation) which are confined to layers just below the solar surface.

The GONG and MDI data can also be used to study latitudinal variations in the properties of the tachocline. By time-averaging the results we find that the tachocline is prolate, with the difference between the tachocline position at 0° and that at 60° latitude being about $(0.020 \pm 0.003)R_\odot$. This is in agreement with results obtained by (Charbonneau et al. 1999). There is also some increase in thickness of the tachocline with latitude, by about $(0.006 \pm 0.002)R_\odot$. This increase is less significant, though still at the 3σ level. We do not find any clear evidence for latitudinal variations in the depth of the convection zone or the extent of overshoot below the convection zone. However, there is a small increase in r_d , the position of the base of the convection zone around the latitude of 60° by $(0.0002 \pm 0.0002)R_\odot$ as compared to the mean value. The significance of this departure is not clear, but it may be noted that Antia et al. (2000a) found a significant excess in sound speed around this latitude, which is concentrated around a radial distance of $0.92R_\odot$. It is quite possible that this has some effect near the base of the convection zone, causing a small difference in r_d . Combining the results on latitudinal variation of the tachocline and the depth of the convection zone, we can conclude that around the solar equator, the bulk of the tachocline is below the base of the convection zone, but at higher latitude a substantial part of the tachocline moves into the convection zone.

The latitudinal dependence of the position of the tachocline will have an important bearing on the theoretical models of the tachocline. Many models are based on the assumption that the tachocline is located in the radiative region. Canuto (1998), however, suggested that buoyancy and vorticity inside the convection zone can account for the small thickness of the tachocline. This model may still be admissible since, at least at high latitudes, about half of the tachocline is inside the convection zone. The thickness of $0.05R_\odot$ for the tachocline as calculated by Canuto, is much larger than what we find, but there is considerable ambiguity in the definition of thickness, since it depends on the actual model of the rotation rate within the tachocline. Furthermore, proper calculations using Canuto's model may even give a different value. So this discrepancy in thickness may not rule out the model. Gough & McIntyre (1998) have proposed that a magnetic field may provide the required horizontal transport to keep the thickness low. However, their estimate of the magnetic field depends on ninth power of the thickness. Considering the ambiguity in the definition of the thickness, it is difficult to draw any conclusions about the validity of this model, but if we use the equatorial value of

the thickness as estimated by us, the required magnetic field turns out to be of the order of 200 G. The physical origin of the prolateness of the tachocline is even more difficult to explain, particularly, since the convection zone itself does not appear to be prolate. A difference between the shape of the tachocline and that of the convection zone base is rather difficult to understand theoretically. It is quite likely that magnetic field, which is estimated to be 10^5 G (D'Silva & Choudhuri 1993) in these layers, plays an important role in determining the shape and thickness of the tachocline as well as its relative position with respect to the convection zone base.

ACKNOWLEDGMENTS

This work utilises data obtained by the Global Oscillation Network Group (GONG) project, managed by the National Solar Observatory, which is operated by AURA, Inc. under a cooperative agreement with the National Science Foundation. The data were acquired by instruments operated by the Big Bear Solar Observatory, High Altitude Observatory, Learmonth Solar Observatory, Udaipur Solar Observatory, Instituto de Astrofísica de Canarias, and Cerro Tololo Interamerican Observatory. This work also utilizes data from the Solar Oscillations Investigation / Michelson Doppler Imager (SOI/MDI) on the Solar and Heliospheric Observatory (SOHO). SOHO is a project of international cooperation between ESA and NASA.

REFERENCES

- Antia H. M., Basu S., 1994, *A&AS*, 107, 421
 Antia H. M., Basu S., 2000, *ApJ*, (in press)
 Antia H. M., Basu S., Chitre S. M., 1998, *MNRAS*, 298, 543
 Antia H. M., Basu S., Hill F., Howe R., Komm R. W., Schou J., 2000a, (preprint)
 Antia H. M., Chitre S. M., Thompson M. J., 2000b, *A&A*, 360, 335
 Basu S., 1997, *MNRAS*, 288, 572
 Basu S., 1998, *MNRAS*, 298, 719
 Basu S., and Antia H. M., 1997, *MNRAS*, 287, 189
 Basu S., and Antia H. M., 2000a, *Solar Phys.*, 192, 449
 Basu S., and Antia H. M., 2000b, *ApJ*, 531, 1088
 Basu S., and Schou J. 2000, *Solar Phys.*, 192, 481
 Basu S., Antia H. M., Narasimha D., 1994, *MNRAS*, 267, 209
 Canuto V. M., 1998, *ApJ*, 497, L51
 Charbonneau P., Christensen-Dalsgaard J., Henning R., Larsen R. M., Schou J., Thompson M. J., Tomczyk S., 1999, *ApJ*, 527, 445
 Christensen-Dalsgaard J., Gough D. O., Thompson, M. J., 1991, *ApJ*, 378, 413
 Corbard T., Berthomieu G., Provost J., Morel P., 1998, *A&A*, 330, 1149
 Corbard T., Blanc-Féraud L., Berthomieu G., Provost J., 1999, *A&A*, 344, 696
 D'Silva S., Choudhuri A. R., 1993, *A&A*, 272, 621
 Gough D. O., 1990, in Osaki Y., Shibahashi H., eds., *Lecture Notes in Physics*, 367, Springer, Berlin, p.283
 Gough D.O., 1993, in Zahn J.-P., Zinn-Justin J., eds., *Astrophysical fluid dynamics*, Les Houches Session XLVII, Elsevier, Amsterdam, p. 399
 Gough D. O., Kosovichev, A. G., 1995, in Hoeksema J. T., Domingo V., Fleck B., Battrick B., eds., *Proc. Fourth SOHO Workshop: Helioseismology*, ESA-SP376 vol. 2; Noordwijk: ESA, p. 47
 Gough D. O., McIntyre M. E., 1998, *Nature*, 394, 755
 Gough D. O., Thompson M. J., 1990, *MNRAS*, 242, 25
 Gough D. O., Thompson M. J., 1991, in Cox A. N., Livingston W. C., Matthews M., eds., *Solar Interior and Atmosphere*, Space Science Series, University of Arizona Press, p. 519
 Gough D. O., Kosovichev A. G., Toomre J., et al., 1996, *Sci*, 272, 1296
 Hill F., Stark P. B., Stebbins R. T., et al., 1996, *Sci*, 272, 1292
 Howe R., Christensen-Dalsgaard J., Hill F., Komm R. W., Larsen R. M., Schou J., Thompson M. J., Toomre J., 2000, *Sci*, 287, 2456
 Kosovichev A. G., 1996, *ApJ*, 469, L61
 Monteiro M. J. P. F. G., Thompson M. J., 1998, in Korzennik S., Wilson A., eds., *Proc: SOHO6/GONG98 workshop, Structure and Dynamics of the Interior of the Sun and Sun-like Stars*, ESA SP-418 (ESA: Noordwijk), p 819
 Monteiro M. J. P. F. G., Christensen-Dalsgaard J., Thompson M. J., 1994, *A&A*, 283, 247
 Monteiro M. J. P. F. G., Christensen-Dalsgaard J., Thompson M. J., 1998, in Korzennik S., Wilson A., eds., *Proc: SOHO6/GONG98 workshop, Structure and Dynamics of the Interior of the Sun and Sun-like Stars*, ESA SP-418 (ESA: Noordwijk), p 495
 Ritzwoller M. H., Lavelly E. M., 1991, *ApJ*, 369, 557
 Schou J., 1999, *ApJ*, 523, L181
 Schou J., Christensen-Dalsgaard J., Thompson M. J., 1994, *ApJ*, 433, 389
 Schou J., Antia H. M., Basu S., et al., 1998, *ApJ*, 505, 390
 Spiegel E. A., Zahn J.-P., 1992, *A&A*, 265, 106
 Thompson M. J., Toomre J., Anderson E. R., et al., 1996, *Sci*, 272, 1300
 Woodard M. F., Libbrecht K. G., 1993, *ApJ*, 402, L77

This paper has been produced using the Royal Astronomical Society/Blackwell Science \TeX macros.